Available online at www.sciencedirect.com
ScienceDirect
Dyes and Pigments 78 (2008) 65–76
DYES and PIGMENTS
www.elsevier.com/locate/dyepig

The synthesis, characterization and properties of coumarin-based chromophores containing a chalcone moiety

Yi-Feng Sun [a,b], Yi- Ping Cui [a,*]

[a] Advanced Photonics Center, School of Electronic Science and Engineering, Southeast University, Nanjing 210096, China
[b] Department of Chemistry, Taishan University, Taian 271021, China

Received 2 August 2007; received in revised form 17 October 2007; accepted 22 October 2007
Available online 7 November 2007

Abstract

A series of coumarin-based derivatives containing a chalcone moiety were synthesized by condensation of 3-acetyl coumarins with aryl or heteroaryl aldehydes in the presence of piperidine in ethanol under microwave irradiation. Structures were established on the basis of ^{1}H NMR, IR, MS and elemental analyses while crystal structure was determined using X-ray diffraction. Absorption and emission spectra showed red-shifts according to the strength of the electron-donating moieties and conjugation length. Replacement of a carbazolyl donor with a triphenylamine group in the coumarinyl-based chromophores resulted in a strong bathochromic shift (1700–1900 cm^{-1}), while the benzocoumarin system caused a bathochromic effect of ~100–500 cm^{-1} relative to the coumarin system.

Keywords: Coumarin derivatives; Chalcone; Crystal structure; Two-photon absorption

1. Introduction

Owing to their attractive applications in materials science and biological imaging, two-photon absorption (TPA) materials have recently received considerable attention [1–3]. The development of new molecules with large TPA cross-sections and efficient up-converted fluorescence at desirable wavelengths plays a crucial role in advancing techniques for laser spectroscopy, laser processing and non-invasive monitoring of diseased tissues. A number of organic molecules have been studied for TPA activity [4–7]. Among these TPA systems, the heterocycle-based chromophores are particularly interesting due to their easily polarizable heteroaromatic rings which can help to improve their degree of intramolecular charge transfer (ICT) [8–10].

As an important group of organic heterocycles, coumarin derivatives are found to possess versatile biological activities [11] and can be found in many natural or synthetic drug molecules. Moreover, their unique photochemical and photophysical properties make them useful in a variety of applications such as in optical brighteners, laser dyes, nonlinear optical chromophores, electroluminescent materials, TPA materials, as well as fluorescent labels and probes in biology and medicine [12–16].

On the other hand, chalcones, the bichromophoric molecules separated by vinyl chains and the carbonyl group, are found be effective photosensitive materials, and exhibit promising nonlinear optical properties [17]. Recent research suggests that the fusion of a chalcone moiety to the coumarin ring appears quite promising for the synthesis of derivatives with enhanced TPA cross-sections [18].

We were especially interested in preparing heteroaromatic derivatives, in particular the coumarin derivatives, both for use as fluorescent labels and probes in biology and medicine and for our studies in efficient TPA-active organic materials. Therefore, based on our previous works [19,20], we wish to report herein the preparation of a series of coumarin-based chromophores containing chalcone moiety under microwave irradiation. At the same time, UV–vis absorption and fluorescence

* Corresponding author.
E-mail addresses: sunyf50@hotmail.com (Y.-F. Sun), cyp@seu.edu.cn (Y.-P. Cui).

0143-7208/$ - see front matter © 2007 Elsevier Ltd. All rights reserved.
doi:10.1016/j.dyepig.2007.10.014

spectra of some selected coumarin derivatives, which contain anthracene, 2-(thiophen-2-yl)thiophene, carbazole, triphenylamine fragments, were measured in solution. Additionally, in order to investigate the real three-dimensional structure of coumarin-based chromophores containing chalcone moiety, the crystals of **1b**, **1e** and **2g** were obtained, and the structures were determined by X-ray diffraction technique. The synthetic pathway and the structures of target molecules are shown in Scheme 1.

2. Experimental

2.1. General

All melting points were determined with a WRS-1A melting point apparatus and are uncorrected. Proton nuclear magnetic resonance (^{1}H NMR) spectra were run on a BrukerAV-600 or AV-400 NMR spectrometer and chemical shifts expressed as δ (parts per million) values with TMS as internal standard. Multiplicities of proton resonance are designated as singlet (s), doublet (d), triplet (t), quartet (q), and multiplet (m). IR spectra were recorded in KBr on a Nicolet NEXUS 470 FT-IR spectrophotometer. Vibrational transition frequencies are reported in wave numbers (cm^{-1}). The UV spectra were recorded using a Varian Cary-100 Bio UV–vis spectrophotometer. The fluorescence spectra were taken with a PE LS50B fluorescence spectrophotometer. Element analysis was taken with a Perkin–Elmer 240 analyzer. Mass spectra (MS) were measured on an API4000 or VG ZAB-HS mass spectrometer. Single crystal was characterized by Bruker Smart 1000 CCD X-ray single crystal diffractometer. All the chemicals are commercially available and they were used without further purification. All the solvents were dried using standard methods before use.

The starting compounds (**1**) were synthesized according to Ref. [21].

2.1.1. 3-Acetyl-2H-1-naphtho[2,1-b]pyran-2-one (*1b*) [21]

^{1}H NMR (400 MHz, $CDCl_3$/TMS) δ: 2.81 (s, 3H), 7.51 (d, $J = 9.0$ Hz, 1H), 7.64 (t, $J = 8.0$ Hz, 1H), 7.78 (t, $J = 8.2$ Hz, 1H), 7.97 (d, $J = 7.9$ Hz, 1H), 8.13 (d, $J = 9.0$ Hz, 1H), 8.41 (d, $J = 8.4$ Hz, 1H), 9.36 (s, 1H).

2.1.2. 3-Acetyl-7-hydroxy-2H-1-benzopyran-2-one (*1c*)

Mp 232–233 °C. ^{1}H NMR (400 MHz, DMSO-d_6/TMS) δ: 2.55 (s, 3H), 6.75 (d, $J = 2.0$ Hz, 1H), 6.85 (dd, $J_1 = 8.4$, $J_2 = 2.0$ Hz, 1H), 7.79 (d, $J = 8.4$ Hz, 1H), 8.59 (s, 1H), 11.12 (s, 1H).

2.1.3. 3-Acetyl-8-methoxy-2H-1-benzopyran-2-one (*1d*)

Mp 172–173 °C. ^{1}H NMR (600 MHz, $CDCl_3$/TMS) δ: 2.74 (s, 3H), 3.99 (s, 3H), 7.19 (dd, $J_1 = 7.8$, $J_2 = 1.2$ Hz, 1H), 7.22 (dd, $J_1 = 7.8$, $J_2 = 1.2$ Hz, 1H), 7.27 (t, $J = 7.8$ Hz, 1H), 8.49 (s, 1H).

2.2. Synthesis of compounds (*2a–u*)

2.2.1. General procedure for conventional heating [22,23]

A mixture of 3-acetyl coumarins (2 mmol), appropriate aryl and heteroaryl aldehydes (2 mmol), and piperidine (0.5 mL) in ethanol (25 mL) was refluxed for 3–5 h and the mixture was monitored by TLC. After cooling, the solid was filtrated and recrystallized from a suitable solvent to afford the pure product.

2.2.2. General procedure for microwave irradiation

To a mixture of 3-acetyl coumarin (2 mmol) and appropriate aryl and heteroaryl aldehydes (2 mmol) in ethanol (30 mL) in a flask, piperidine (0.3 mL) in ethanol (5 mL) was added dropwise. The mixture was irradiated in a Galanz microwave oven for an optimized time and taken out for a few seconds and at the same time, the mixture was stirred carefully using a bar. The mixture was subjected to microwave irradiation

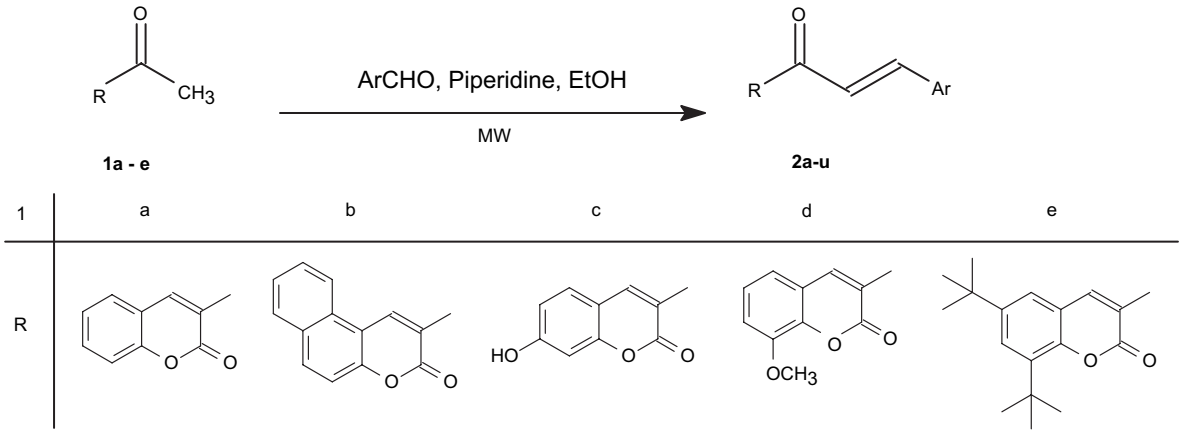

2a R = d, Ar = 4-N,N-dimethylaminophenyl; **2b** R = e, Ar = 4-N,N-dimethylaminophrnyl; **2c** R = c, Ar = 9-anthryl; **2d** R = d, Ar = 9-anthryl; **2e** R = e, Ar = 9-anthryl; **2f** R = a, Ar = 4-N,N-diphenylaminophenyl; **2g** R = b, Ar = 4-N,N-diphenylaminophenyl; **2h** R = d, Ar = 4-N,N-diphenylaminophenyl; **2i** R = d, Ar = 1H-indol-3-yl; **2j** R = e, Ar = 1H-indol-3-yl; **2k** R = a, Ar = benzofran-2-yl; **2l** R = d, Ar = benzofran-2-yl; **2m** R = e, Ar = ben -zofran-2-yl; **2n** R = a, Ar = benzothiophen-3-yl; **2o** R = d, Ar = benzothiophen-3-yl; **2p** R = a, Ar = 2-(thiophen-2-yl) thiophen-5-yl; **2q** R = b, Ar = 2-(thiophen-2-yl) thiophen-5-yl; **2r** R = e, Ar = 2-(thiophen-2-yl) thiophen-5-yl; **2s** R = a, Ar = N-ethyl-3-carbazolyl; **2t** R = b, Ar = N-ethyl-3-carbazolyl; **2u** R = d, Ar = N-ethyl-3-carbazolyl.

Scheme 1. The synthetic pathway and the structures of target molecules.

for another optimized time and then taken out for stirring. The operation was repeated several times, and the reaction mixture was monitored by TLC. After the reaction was completed, the reaction mixture was cooled to room temperature. The precipitate was filtrated and recrystallized form EtOH–CH_3COCH_3 or EtOH–DMF.

*2.2.2.1. 8-Methoxy-3-(3-(4-N,N-dimethylaminophenyl)prop-2-enoyl)-2H-1-benzopyran-2-one (**2a**).* Yield 69%; mp 184–185 °C. ^{1}H NMR (400 Hz, $CDCl_3$/TMS) δ: 3.06 (s, 6H), 4.00 (s, 3H), 6.74 (d, $J = 6.8$ Hz, 2H), 7.15–7.29 (m, 3H), 7.60 (d, $J = 9.0$ Hz, 2H), 7.76 (d, $J = 15.6$ Hz, 1H), 7.88 (d, $J = 15.6$ Hz, 1H), 8.55 (s, 1H). MS *m/z*: 350.4 (M + 1). Anal. calcd for $C_{21}H_{19}NO_4$: C 72.19, H 5.48, N 4.01; found: C 72.12, H 5.57, N 4.06.

*2.2.2.2. 6,8-Di-tert-butyl-3-(3-(4-N,N-dimethylaminophenyl)-prop-2-enoyl)-2H-1-benzopyran-2-one (**2b**).* Yield 77%; mp 239–240 °C. ^{1}H NMR (400 Hz, $CDCl_3$/TMS) δ: 1.37 (s, 9H), 1.54 (s, 9H), 3.06 (s, 6H), 6.73 (d, $J = 6.8$ Hz, 2H), 7.46 (d, $J = 2.4$ Hz, 1H), 7.61 (d, $J = 8.8$ Hz, 1H), 7.67 (d, $J = 2.2$ Hz, 1H), 7.84 (d, $J = 15.6$ Hz, 1H), 7.88 (d, $J = 15.6$ Hz, 1H), 8.58 (s, 1H). IR (KBr) ν: 1725, 1655, 1609, 1577 cm^{-1}. MS *m/z*: 432.7 (M + 1). Anal. calcd for $C_{28}H_{33}NO_3$: C 77.93, H 7.71, N 3.25; found: C 78.02, H 7.79, N 3.13.

*2.2.2.3. 7-Hydroxy-3-(3-(9-anthryl)prop-2-enoyl)-2H-1-benzopyran-2-one (**2c**).* Yield 62%; mp >255 °C. ^{1}H NMR (DMSO-d_6/TMS) δ: 6.78 (d, $J = 2.0$ Hz, 1H), 6.89 (dd, $J = 9.0$, 2.0 Hz, 1H), 7.55–7.62 (m, 4H), 7.69 (d, $J = 16.0$ Hz, 1H), 7.84 (d, $J = 9.0$ Hz, 1H), 8.15 (d, $J = 9.0$ Hz, 2H), 8.35 (dd, $J = 9.0$, 1.0 Hz, 2H), 8.62 (d, $J = 16.0$ Hz, 1H), 8.68 (s, 1H), 8.76 (s, 1H), 11.20 (s, 1H). IR (KBr) ν: 1706, 1597, 1550 cm^{-1}. FAB-MS *m/z*: 393 (M + 1). Anal. calcd for $C_{26}H_{16}O_4$: C 79.58, H 4.11; found: C 79.36, H 4.05.

*2.2.2.4. 8-Methoxy-3-(3-(9-anthryl)prop-2-enoyl)-2H-1-benzopyran-2-one (**2d**).* Yield 65%; mp 219–220 °C. ^{1}H NMR (400 Hz, $CDCl_3$/TMS) δ: 3.99 (s, 3H), 7.19–7.58 (m, 7H), 7.85 (d, $J = 16.0$ Hz, 1H), 8.03 (d, $J = 8.4$ Hz, 1H), 8.42 (d, $J = 8.4$ Hz, 1H), 8.49 (s, 1H), 8.64 (s, 1H), 8.86 (d, $J = 16.0$ Hz, 1H). FAB-MS *m/z*: 407 (M + 1). Anal. calcd for $C_{27}H_{18}O_4$: C 79.79, H 4.46; found: C 79.82, H 4.53.

*2.2.2.5. 6,8-Di-tert-butyl-3-(3-(9-anthryl)prop-2-enoyl)-2H-1-benzopyran-2-one (**2e**).* Yield 86%; mp 204–205 °C. ^{1}H NMR (400 Hz, DMSO-d_6/TMS) δ: 1.35 (s, 9H), 1.49 (s, 9H), 7.59–7.66 (m, 5H), 7.69 (d, $J = 2.4$ Hz, 1H), 7.91 (d, $J = 2.4$ Hz, 1H), 8.17 (d, $J = 8.8$ Hz, 2H), 8.37 (d, $J = 8.8$ Hz, 2H), 8.68 (d, $J = 16.4$ Hz, 1H), 8.72 (s, 1H), 8.83 (s, 1H). IR (KBr) ν: 1720, 1662, 1609, 1582 cm^{-1}. ESI-MS *m/z*: 489.2430 (M + 1). Anal. calcd for $C_{34}H_{32}O_3$: C 83.58, H 6.60; found: C 83.51, H 6.65.

*2.2.2.6. 3-(3-(4-N,N-Diphenylaminophenyl)prop-2-enoyl)-2H-1-benzopyran-2-one (**2f**).* Yield 80%; mp 189–190 °C. ^{1}H NMR (600 Hz, $CDCl_3$/TMS) δ: 7.03 (d, $J = 8.7$ Hz, 2H), 7.13 (t, $J = 7.4$ Hz, 2H), 7.16 (d, $J = 8.4$ Hz, 4H), 7.31–7.38 (m, 5H), 7.41 (d, $J = 8.3$ Hz, 1H), 7.54 (d, $J = 8.7$ Hz, 2H), 7.67 (m, 2H), 7.81 (d, $J = 15.6$ Hz, 1H), 7.87 (d, $J = 15.6$ Hz, 1H), 8.60 (s, 1H). IR (KBr) ν: 1720, 1650, 1606, 1588 cm^{-1}. MS *m/z*: 444.6 (M + 1). Anal. calcd for $C_{30}H_{21}NO_3$: C 81.25, H 4.77, N 3.16; found: C 81.13, H 4.85, N 3.04.

*2.2.2.7. 3-(3-(4-N,N-Diphenylaminophenyl)prop-2-enoyl)-2H-1-naphtho[2,1-b]pyran-2-one (**2g**).* Yield 83%; mp 237–239 °C. ^{1}H NMR (400 Hz, $CDCl_3$/TMS) δ: 7.04 (d, $J = 8.3$ Hz, 2H), 7.11–7.19 (m, 6H), 7.33 (t, $J = 7.7$ Hz, 4H), 7.52 (d, $J = 9.0$ Hz, 1H), 7.57 (d, $J = 8.4$ Hz, 2H), 7.64 (t, $J = 7.4$ Hz, 1H), 7.78 (t, $J = 7.4$ Hz, 1H), 7.91 (d, $J = 15.5$ Hz, 1H), 7.95 (d, $J = 7.3$ Hz, 1H), 7.97 (d, $J = 15.7$ Hz, 1H), 8.00–8.03 (m, 3H), 8.12 (d, $J = 9.0$ Hz, 1H), 8.44 (d, $J = 8.3$ Hz, 1H), 9.43 (s, 1H). MS *m/z*: 494.6 (M + 1). Anal. calcd for $C_{34}H_{23}NO_3$: C 82.74, H 4.70, N 2.84; found: C 82.91, H 4.67, N 2.88.

*2.2.2.8. 8-Methoxy-3-(3-(4-N,N-diphenylaminophenyl)prop-2-enoyl)-2H-1-benzopyran-2-one (**2h**).* Yield 78%; mp 226–228 °C. ^{1}H NMR (600 Hz, DMSO-d_6/TMS) δ: 3.95 (s, 3H), 6.91 (d, $J = 8.6$ Hz, 2H), 7.12 (d, $J = 7.7$ Hz, 4H), 7.16 (t, $J = 7.4$ Hz, 2H), 7.35–7.38 (m, 5H), 7.43 (d, $J = 8.7$ Hz, 1H), 7.46–7.49 (m, 2H), 7.63 (d, $J = 8.6$ Hz, 2H), 7.69 (d, $J = 15.8$ Hz, 1H), 8.60 (s, 1H). FAB-MS *m/z*: 474 (M + 1). Anal. calcd for $C_{31}H_{23}NO_4$: C 78.63, H 4.90, N 2.96; found: C 78.73, H 5.01, N 3.87.

*2.2.2.9. 8-Methoxy-3-(3-(1H-indol-3-yl)prop-2-enoyl)-2H-1-benzopyran-2-one (**2i**).* Yield 71%; mp 251–252 °C. ^{1}H NMR (400 Hz, DMSO-d_6/TMS) δ: 3.96 (s, 3H), 7.22–7.52 (m, 6H), 7.67 (d, $J = 15.6$ Hz, 1H), 7.69–7.99 (m, 1H), 8.04 (d, $J = 16.0$ Hz, 1H), 8.07 (s, 1H), 8.62 (s, 1H), 11.96 (s, 1H). IR (KBr) ν: 3253, 1729, 1643, 1610, 1572 cm^{-1}. MS *m/z*: 346.4 (M + 1). Anal. calcd for $C_{21}H_{15}NO_4$: C 73.04, H 4.38, N 4.06; found: C 73.18, H 4.46, N 3.95.

*2.2.2.10. 6,8-Di-tert-butyl-3-(3-(1H-indol-3-yl)prop-2-enoyl)-2H-1-benzopyran-2-one (**2j**).* Yield 81%; mp 247–248 °C. ^{1}H NMR (400 Hz, DMSO-d_6/TMS) δ: 1.35 (s, 9H), 1.51 (s, 9H), 7.25–7.53 (m, 2H), 7.67 (d, $J = 2.0$ Hz, 1H), 7.82 (d, $J = 15.6$ Hz, 1H), 7.86 (d, $J = 2.4$ Hz, 1H), 7.99–8.02 (m, 1H), 8.06 (d, $J = 15.6$ Hz, 1H), 8.07 (d, $J = 2.4$ Hz, 1H), 8.70 (s, 1H). IR (KBr) ν: 3242, 1732, 1722, 1638, 1609, 1576 cm^{-1}. MS *m/z*: 428.2239 (M + 1). Anal. calcd for $C_{28}H_{29}NO_3$: C 78.66, H 6.84, N 3.28; found: C 78.53, H 6.92, N 3.25.

*2.2.2.11. 3-(3-(Benzofuran-2-yl)prop-2-enoyl)-2H-1-benzopyran-2-one (**2k**).* Yield 64%; mp 196–197 °C. ^{1}H NMR (400 Hz, $CDCl_3$/TMS) δ: 7.09 (s, 1H), 7.23–7.43 (m, 4H), 7.54 (d, $J = 8.4$ Hz, 1H), 7.61 (d, $J = 7.6$ Hz, 1H), 7.65–7.70 (m, 2H), 7.75 (d, $J = 15.2$ Hz, 1H), 8.04 (d, $J = 15.2$ Hz, 1H), 8.60 (s, 1H). IR (KBr) ν: 1734, 1655, 1610, 1582 cm^{-1}. MS *m/z*: 317.4

(M + 1). Anal. calcd for $C_{20}H_{12}O_4$: C 75.94, H 3.82; found: C 75.83, H 3.76.

*2.2.2.12. 8-Methoxy-3-(3-(benzofuran-2-yl)prop-2-enoyl)-2H-1-benzopyran-2-one (**2l**).* Yield 68%; mp 205–207 °C. ^{1}H NMR (600 Hz, $CDCl_3$/TMS) δ: 4.03 (s, 3H), 7.10 (s, 1H), 7.21–7.32 (m, 4H), 7.41 (t, $J = 8.3$ Hz, 1H), 7.55 (d, $J = 8.3$ Hz, 1H), 7.62 (d, $J = 7.7$ Hz, 1H), 7.76 (d, $J = 15.4$ Hz, 1H), 8.05 (d, $J = 15.4$ Hz, 1H), 8.59 (s, 1H). IR (KBr) ν: 1732, 1657, 1608, 1584 cm^{-1}. MS *m/z*: 347.3 (M + 1). Anal. calcd for $C_{21}H_{14}O_5$: C 72.83, H 4.07; found: C 72.87, H 4.15.

*2.2.2.13. 6,8-Di-tert-butyl-3-(3-(benzofuran-2-yl)prop-2-enoyl)-2H-1-benzopyran-2-one (**2m**).* Yield 76%; mp 194–195 °C. ^{1}H NMR (600 Hz, $CDCl_3$/TMS) δ: 1.39 (s, 9H), 1.56 (s, 9H), 7.09 (s, 1H), 7.25 (t, $J = 8.7$ Hz, 1H), 7.40 (t, $J = 7.8$ Hz, 1H), 7.49 (d, $J = 2.2$ Hz, 1H), 7.53 (d, $J = 8.3$ Hz, 1H), 7.62 (d, $J = 7.8$ Hz, 1H), 7.72 (d, $J = 2.2$ Hz, 1H), 7.76 (d, $J = 15.4$ Hz, 1H), 8.14 (d, $J = 15.4$ Hz, 1H), 8.62 (s, 1H). IR (KBr) ν: 1731, 1659, 1612, 1573 cm^{-1}. MS *m/z*: 429.5 (M + 1). Anal. calcd for $C_{28}H_{28}O_4$: C 78.48, H 6.59; found: C 78.55, H 6.51.

*2.2.2.14. 3-(3-(Benzothiophen-3-yl)prop-2-enoyl)-2H-1-benzopyran-2-one (**2n**).* Yield 75%; mp 204–205 °C. ^{1}H NMR (600 Hz, $CDCl_3$/TMS) δ: 7.39 (t, $J = 7.6$ Hz, 1H), 7.42–7.47 (m, 2H), 7.53 (t, $J = 8.0$ Hz, 1H), 7.69 (t, $J = 8.6$ Hz, 1H), 7.72 (d, $J = 7.7$ Hz, 1H), 7.92 (d, $J = 8.0$ Hz, 1H), 8.01 (s, 1H), 8.13 (d, $J = 15.8$ Hz, 1H), 8.19 (d, $J = 15.4$ Hz, 1H), 8.20 (d, $J = 8.9$ Hz, 1H), 8.67 (s, 1H). FAB-MS *m/z*: 333 (M + 1). Anal. calcd for $C_{20}H_{12}O_3S$: C 72.27, H 3.64; found: C 72.34, H 3.67.

*2.2.2.15. 8-Methoxy-3-(3-(benzothiophen-3-yl)prop-2-enoyl)-2H-1-benzopyran-2-one (**2o**).* Yield 71%; mp 251–252 °C. ^{1}H NMR (600 Hz, $CDCl_3$/TMS) δ: 4.02 (s, 3H), 7.22 (d, $J = 7.6$ Hz, 1H), 7.28–7.33 (m, 2H), 7.45 (t, $J = 7.5$ Hz, 1H), 7.52 (t, $J = 7.6$ Hz, 1H), 7.92 (d, $J = 8.0$ Hz, 1H), 8.01 (s, 1H), 8.13 (d, $J = 15.8$ Hz, 1H), 8.19 (d, $J = 15.3$ Hz, 1H), 8.20 (d, $J = 8.8$ Hz, 1H), 8.64 (s, 1H). FAB-MS *m/z*: 363 (M + 1). Anal. calcd for $C_{21}H_{14}O_4S$: C 69.60, H 3.89; found: C 69.67, H 3.83.

*2.2.2.16. 3-(3-(2-(Thiophen-2-yl)thiophen-5-yl)prop-2-enoyl)-2H-1-benzopyran-2-one (**2p**).* Yield 75%; mp 208–209 °C. ^{1}H NMR (400 Hz, $CDCl_3$/TMS) δ: 7.06 (d, $J = 4.4$ Hz, 1H), 7.16 (d, $J = 4.0$ Hz, 1H), 7.28–7.32 (m, 3H), 7.36 (t, $J = 7.6$ Hz, 1H), 7.41 (d, $J = 8.4$ Hz, 1H), 7.64–7.69 (m, 2H), 7.72 (d, $J = 15.6$ Hz, 1H), 7.96 (d, $J = 15.2$ Hz, 1H), 8.60 (s, 1H). IR (KBr) ν: 1725, 1653, 1612, 1570 cm^{-1}. FAB-MS *m/z*: 365 (M + 1). Anal. calcd for $C_{20}H_{12}O_3S_2$: C 65.92, H 3.32; found: C 65.83, H 3.41.

*2.2.2.17. 3-(3-(2-(Thiophen-2-yl)thiophen-5-yl)prop-2-enoyl)-2H-1-naphtho[2,1-b]pyran-2-one (**2q**).* Yield 69%; mp 244–246 °C. ^{1}H NMR (400 Hz, $CDCl_3$/TMS) δ: 7.08 (t, $J = 4.3$ Hz, 1H), 7.19 (d, $J = 3.8$ Hz, 1H), 7.31–7.36 (m, 3H), 7.54 (d, $J = 9.0$ Hz, 1H), 7.65 (t, $J = 7.5$ Hz, 1H), 7.79 (t, $J = 7.7$ Hz, 1H), 7.87 (d, $J = 15.3$ Hz, 1H), 7.96 (d, $J = 8.0$ Hz, 1H), 8.02 (d, $J = 15.3$ Hz, 1H), 8.14 (d, $J = 9.0$ Hz, 1H), 8.45 (d, $J = 8.5$ Hz, 1H), 9.45 (s, 1H). FAB-MS *m/z*: 415 (M + 1). Anal. calcd for $C_{24}H_{14}O_3S_2$: C 69.55, H 3.40; found: C 69.67, H 3.48.

*2.2.2.18. 6,8-Di-tert-butyl-3-(3-(2-(thiophen-2-yl)thiophen-5-yl)prop-2-enoyl)-2H-1-benzopyran-2-one (**2r**).* Yield 72%; mp 161–162 °C. ^{1}H NMR (400 Hz, $CDCl_3$/TMS) δ: 1.37 (s, 9H), 1.54 (s, 9H), 7.06 (t, $J = 4.4$ Hz, 1H), 7.16 (d, $J = 4.4$ Hz, 1H), 7.26–7.30 (m, 3H), 7.48 (d, $J = 2.4$ Hz, 1H), 7.69 (d, $J = 2.0$ Hz, 1H), 7.82 (d, $J = 15.2$ Hz, 1H), 7.95 (d, $J = 15.2$ Hz, 1H), 8.61 (s, 1H). IR (KBr) ν: 1729, 1655, 1609, 1583 cm^{-1}. FAB-MS *m/z*: 477 (M + 1). Anal. calcd for $C_{28}H_{28}O_3S_2$: C 70.55, H 5.92; found: C 70.63, H 5.81.

*2.2.2.19. 3-(3-(N-Ethyl-3-carbazolyl)prop-2-enoyl)-2H-1-benzopyran-2-one (**2s**).* Yield 78%; mp 207–208 °C. ^{1}H NMR (400 Hz, $CDCl_3$/TMS) δ: 1.46 (t, $J = 7.2$ Hz, 3H), 4.38 (q, $J = 7.2$ Hz, 2H), 7.27–7.37 (m, 2H), 7.40–7.51 (m, 4H), 7.63–7.69 (m, 2H), 7.85 (d, $J = 8.4$ Hz, 1H), 8.01 (d, $J = 15.6$ Hz, 1H), 8.14 (d, $J = 15.2$ Hz, 1H), 8.16 (d, $J = 8.8$ Hz, 1H), 8.41 (s, 1H), 8.61 (s, 1H). IR (KBr) ν: 1732, 1659, 1613, 1570 cm^{-1}. MS *m/z*: 394.3 (M + 1). Anal. calcd for $C_{26}H_{19}NO_3$: C 79.37, H 4.87, N 3.56; found: C 79.53, H 4.81, N 3.45.

*2.2.2.20. 3-(3-(N-Ethyl-3-carbazolyl)prop-2-enoyl)-2H-1-naphtho[2,1-b]pyran-2-one (**2t**).* Yield 83%; mp 241–242 °C. ^{1}H NMR (400 Hz, $CDCl_3$/TMS) δ: 1.49 (t, $J = 7.2$ Hz, 3H), 4.42 (q, $J = 7.2$ Hz, 2H), 7.32 (t, $J = 7.4$ Hz, 1H), 7.45 (d, $J = 8.7$ Hz, 2H), 7.51–7.57 (m, 2H), 7.65 (t, $J = 7.5$ Hz, 1H), 7.79 (t, $J = 7.5$ Hz, 1H), 7.91 (d, $J = 8.4$ Hz, 1H), 7.97 (d, $J = 8.1$ Hz, 1H), 8.12–8.26 (m, 4H), 8.46 (s, 1H), 8.48 (d, $J = 8.5$ Hz, 1H), 9.48 (s, 1H). MS *m/z*: 444.5 (M + 1). Anal. calcd for $C_{30}H_{21}NO_3$: C 81.25, H 4.77, N 3.16; found: C 81.37, H 4.64, N 3.25.

*2.2.2.21. 8-Methoxy-3-(3-(N-ethyl-3-carbazolyl)prop-2-enoyl)-2H-1-benzopyran-2-one (**2u**).* Yield 82%; mp 247–248 °C. ^{1}H NMR (600 Hz, $CDCl_3$/TMS) δ: 1.48 (t, $J = 7.3$ Hz, 3H), 4.03 (s, 3H), 4.41 (q, $J = 7.3$ Hz, 2H), 7.20 (d, $J = 7.7$ Hz, 1H), 7.25–7.33 (m, 3H), 7.44 (t, $J = 8.6$ Hz, 2H), 7.52 (t, $J = 7.5$ Hz, 1H), 7.87 (d, $J = 8.5$ Hz, 1H), 8.02 (d, $J = 15.5$ Hz, 1H), 8.15 (d, $J = 15.5$ Hz, 1H), 8.16 (d, $J = 7.6$ Hz, 1H), 8.42 (s, 1H), 8.60 (s, 1H). IR (KBr) ν: 1732, 1653, 1610, 1576 cm^{-1}. MS *m/z*: 424.5 (M + 1). Anal. calcd for $C_{27}H_{21}NO_4$: C 76.58, H 5.00, N 3.31; found: C 76.52, H 4.87, N 3.23.

2.3. X-ray crystallography

Suitable single crystals of **1b**, **1e** and **2g** for X-ray structural analysis were obtained by evaporation of ethanol–acetone, ethanol and ethyl acetate solution, respectively. The diffraction

data were collected with a Bruker Smart Apex 1000 CCD area detector using a graphite monochromated Mo Kα radiation ($\lambda = 0.71073$ Å) at 273 (2) K. The structures were solved by direct methods with SHELXS-97 program and refinements on F^2 were performed with SHELXL-97 program by full-matrix least-squares techniques with anisotropic thermal parameters for the non-hydrogen atoms. All hydrogen atoms were added according to a theoretical model. A summary of the crystallographic data and structure refinement details is given in Table 1.

3. Results and discussion

3.1. Synthesis

The required 3-acetyl coumarins **1** were prepared from substituted salicylaldehyde with ethyl acetoacetate according to the method reported in literature [21]. Coumarin derivatives **2** were readily synthesized by refluxing 3-acetyl coumarins with various aryl or heteroaryl aldehydes in the presence of piperidine in ethanol. The same condensation between 3-acetyl coumarin and aldehydes could be carried out under microwave conditions. It is noteworthy that the reaction which required 3–5 h in conventional method, was completed efficiently, with 62–86% yields, in 2–10 min under microwave conditions (Scheme 1). Therefore, the microwave procedure could offer an efficient pathway to attach anthracene, 2-(thiophen-2-yl)-thiophene, carbazole, triphenylamine fragments to the 3-position of coumarin derivatives.

All the synthesized compounds (**2**) have been characterized on the basis of their physical data and spectral analysis. These compounds show the band at 1706–1734 cm^{-1} for typical lactone carbonyl group. All the compounds show the NMR signals for different kinds of protons at their respective positions. The values are consistent with their predicted structures (Scheme 1).

3.2. Crystal structures

Although compound **1b** has been studied previously by other groups, the crystal structure of **1b** has not been reported. As can be seen from Fig. 1, the molecule of **1b** is essentially planar with maximum deviations of −0.0947 Å for atom O1. This is obviously different from the situation in 3-acetyl-7-methoxycoumarin [24], in which the plane of the acetyl substituent is rotated by 12.26(9)° from the molecular plane. There is

Table 1
Crystal data and structure refinement[a]

Compound	**1b**	**1e**	**2g**
Empirical formula	$C_{15}H_{10}O_3$	$C_{19}H_{24}O_3$	$C_{34}H_{23}NO_3$
Formula weight	238.23	300.38	493.53
Temperature (K)	273(2)	273(2)	273(2)
Crystal system	Monoclinic	Triclinic	Triclinic
Space group	$P2_1/c$	$P\bar{1}$	$P\bar{1}$
Unit cell dimensions			
a (Å)	5.5302(9)	9.898(2)	7.9248(3)
b (Å)	9.2841(15)	12.826(3)	9.1581(3)
c (Å)	21.362(4)	15.500(3)	19.1055(7)
α (°)	90	69.823(3)	80.8950(10)
β (°)	92.368(2)	74.340(4)	82.8720(10)
γ (°)	90	77.408(4)	66.4090(10)
Volume (Å^3), Z	1095.9(3), 4	1761.4(6), 4	1251.88(8), 2
D_{calc} (Mg/m^3)	1.444	1.133	1.309
Absorption coefficient (mm^{-1})	0.101	0.075	0.083
F (0 0 0)	496	648	516
Crystal size (mm)	0.75 × 0.54 × 0.20	0.25 × 0.25 × 0.20	0.25 × 0.20 × 0.17
θ Range for data collection (°)	2.39–24.99	2.16–25.05	1.08–25.00
Limiting indices	$-6 \le h \le 6$	$-11 \le h \le 11$	$-9 \le h \le 9$
	$-8 \le k \le 11$	$-13 \le k \le 15$	$-10 \le k \le 10$
	$-23 \le l \le 25$	$-18 \le l \le 17$	$-22 \le l \le 22$
Reflections collected/unique	3747/1616 [$R_{int} = 0.0106$]	7425/6198 [$R_{int} = 0.0120$]	14 370/4391 [$R_{int} = 0.0285$]
Max. and min. transmissions	0.9801 and 0.9282	0.9851 and 0.9815	0.9860 and 0.9794
Data/restraints/parameters	1616/0/163	6198/0/412	4391/0/344
Goodness-of-fit on F^2	1.002	1.018	1.087
Final R indices [$I > 2$sigma(I)]	$R_1 = 0.0582$	$R_1 = 0.0590$	$R_1 = 0.0377$
	$wR_2 = 0.1485$	$wR_2 = 0.1606$	$wR_2 = 0.1033$
R Indices (all data)	$R_1 = 0.0773$	$R_1 = 0.0736$	$R_1 = 0.0493$
	$wR_2 = 0.1965$	$wR_2 = 0.1702$	$wR_2 = 0.1193$
Extinction coefficient		0.0059(15)	0.036(3)
Largest diff. peak and hole (e Å^{-3})	0.208 and −0.327	0.541 and −0.285	0.152 and −0.165
CCDC	649893	649894	649895

[a] In all cases the X-ray wavelength was 0.71073 Å, correction for absorption was semi-empirical from equivalent reflections and the refinement method was full-matrix least-squares on F^2.

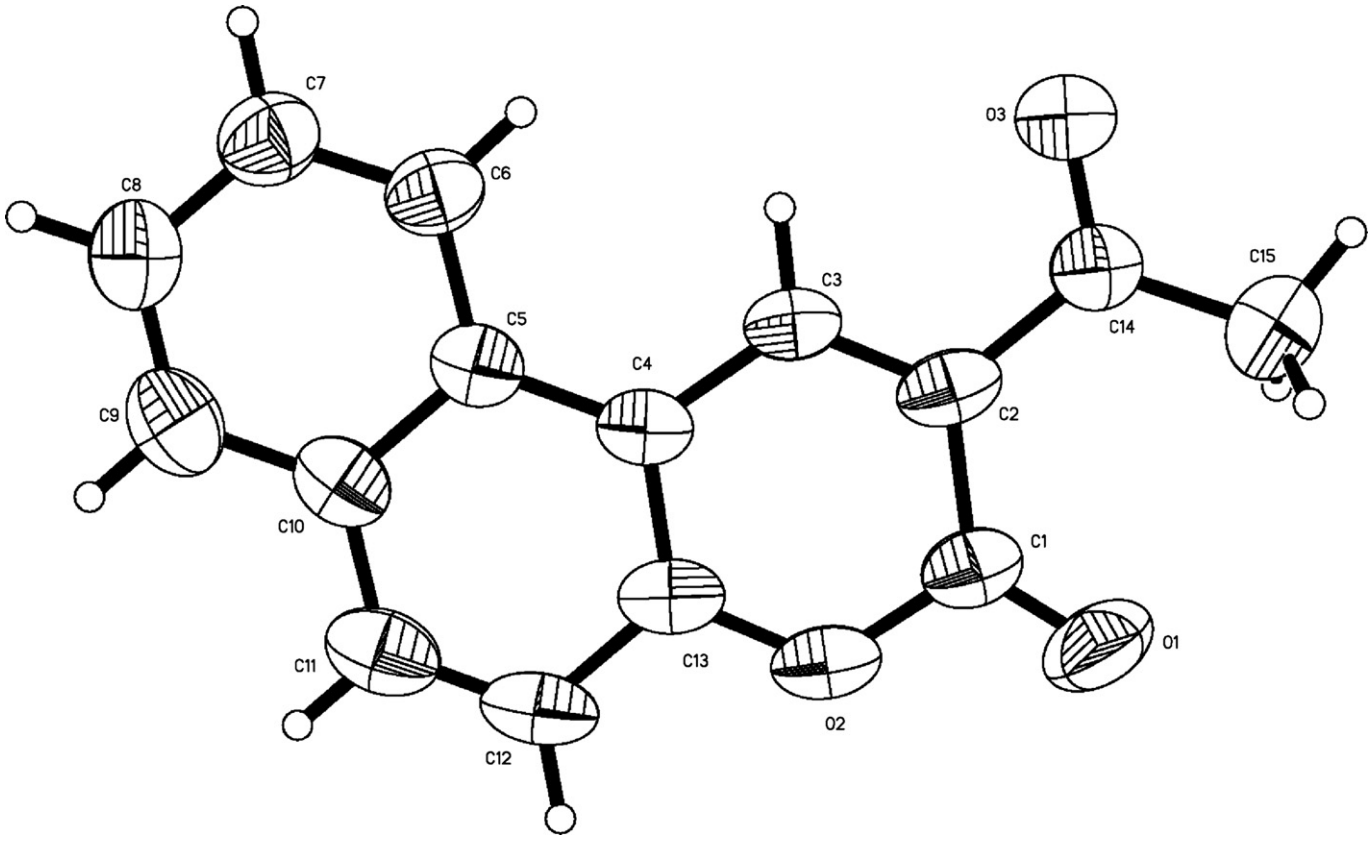

Fig. 1. The molecular structure of **1b**, showing the atom-labelling scheme. Displacement ellipsoids are drawn at the 50% probability level. H atoms are shown as small spheres of arbitrary radius.

an intermolecular π−π stacking interaction between the **1b** molecules in crystal lattice as shown in Fig. 2.

The structure of **1e** is shown in Fig. 3. There are two crystallographically independent but conformationally almost identical molecules in the asymmetric unit. The bond geometries show good agreement between molecules A (C1−C9) and B (C20−C28). However, they differ with respect to torsion angle. As a result, the dihedral angle between the coumarin ring plane and the acetyl group plane in A is 16°, obviously larger than the value of 7.7° found in B, but close to the reported value of 12.26(9)° [24]. Moreover, in each molecule, the coumarin moiety deviates only slightly from being fully planar.

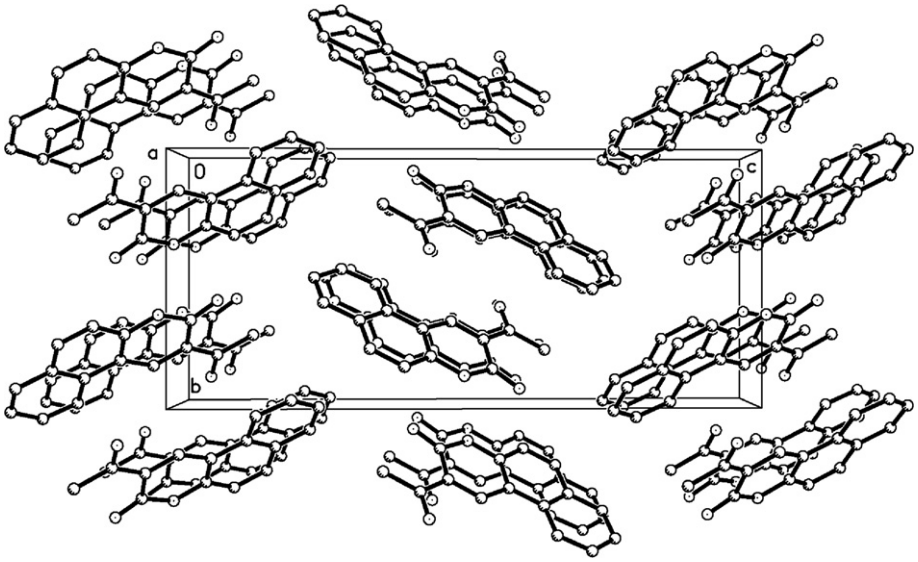

Fig. 2. The packing diagram along *a*-axis of **1b**. H atoms are omitted for clarity.

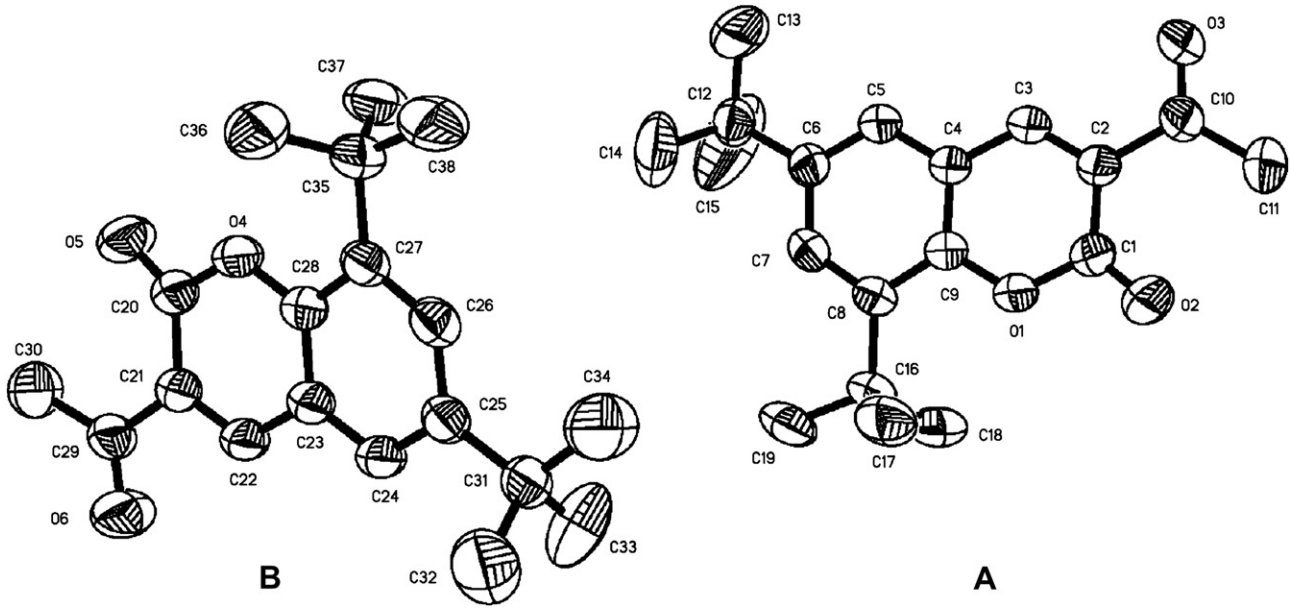

Fig. 3. The molecular structure of **1e**, showing the atom-labelling scheme. Displacement ellipsoids are drawn at the 50% probability level. H atoms are omitted for clarity.

Like molecule **1b**, in **2g** also, the coumarin core has a planar conformation (Fig. 4). The dihedral angle between the lactone and naphthalene rings is 4°, indicating their mean planarity. However, molecule **2g** is not planar and adopts a *trans* configuration about the central olefinic bond. The benzocoumarin system and C17 phenyl ring make a dihedral angle of 30.8°, and are twisted out of the plane of the central chalcone unit on the same side (Fig. 5). Therefore, apart from the two phenyl rings (C23 and C29), the rest of the molecule exhibits a bent-planar configuration, as observed in DASTA [25]. But the latter has more tiny curvature. This is in marked contrast to the orientations in **2e** (Fig. 6), which were reported previously [26], in which the anthracene ring is rotated significantly out of the plane of the rest of the molecule (Fig. 7). On the other hand, the three aryl rings of the triphenylamine moiety show no coplanar structure. At the diphenylamino donor end, the central nitrogen and its three bended carbon atoms are basically coplanar, forming a quasi-equilateral trigonal NC3 plane, with the sum of the three C–N–C angles (359.82°) being very close to 360°. Around the central nitrogen, three phenyl ring planes are arranged in a propeller-like fashion. The linkage between 3-carbonyl-5,6-benzo-coumarin system and phenyl ring (C17) is quite conjugated with bond lengths of C14–C15: 1.458 Å, C15–C16: 1.326 Å and C16–C17: 1.452 Å, suggesting that all non-hydrogen atoms between donor and acceptor are highly conjugated, leading to a π-bridge for the charge

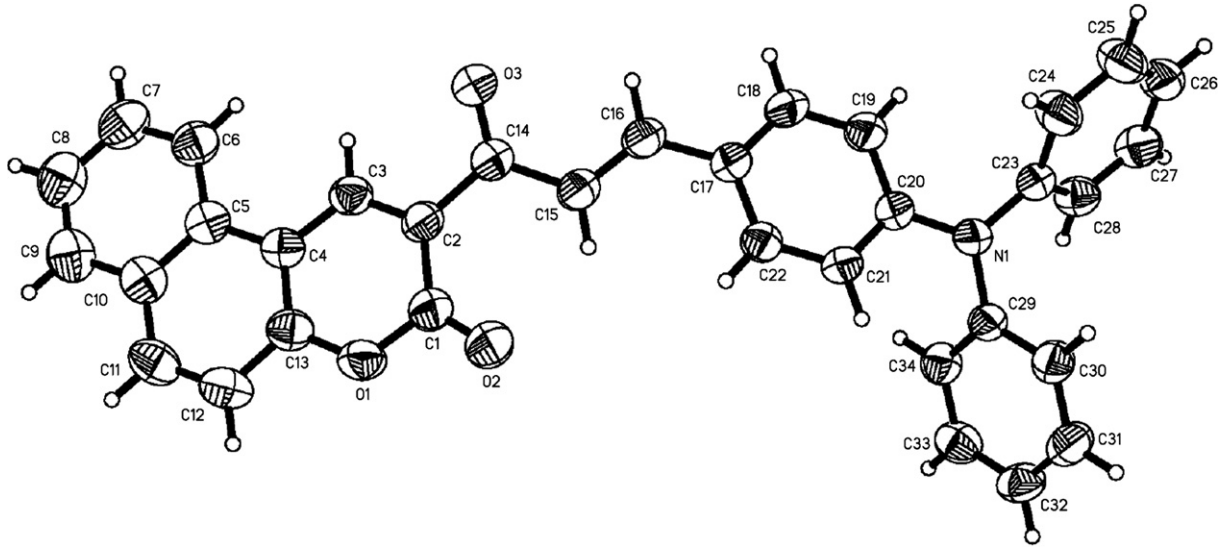

Fig. 4. The molecular structure of **2g**, showing the atom-labelling scheme. Displacement ellipsoids are drawn at the 50% probability level. H atoms are shown as small spheres of arbitrary radius.

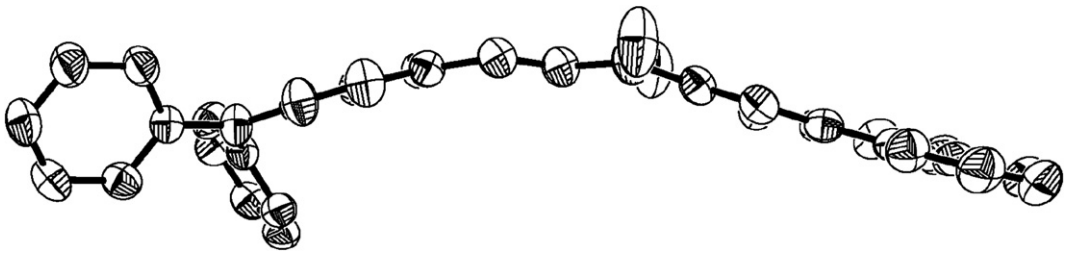

Fig. 5. The side elevation of **2g**. H atoms are omitted for clarity.

transfer from amino to 3-carbonyl-5,6-benzocoumarin system. Similar geometry has been observed in related triarylamine analogues [27,28]. In addition, there is also an intermolecular π–π stacking interaction between **2g** molecules in crystal lattice as shown in Fig. 8.

3.3. Absorption and fluorescence spectra

The molecular structures of the coumarinyl-based organic molecules investigated are shown in Fig. 9. These molecules consist of a typical A–π–D structure, where 3-carbonylcoumarinyl, vinyl and carbazolyl (or triphenylamine, anthryl and 2-(thiophen-2-yl)thiophene) groups are employed as acceptor (A), π-conjugated center (π) and donor (D) moieties, respectively. As seen from Fig. 9, structural modification occurs only in one terminal moiety, where a carbazolyl donor was replaced by a triphenylamine or 2-(thiophen-2-yl)thiophene group, or a 3-carbonylcoumarin acceptor was replaced by a 3-carbonyl-5,6-benzocoumarin acceptor. Such a modification could be expected to result in notable changes in the π-conjugated length and red-shifts in the absorption and emission spectra.

UV–vis absorption spectra of these molecules in diluted chloroform solutions are given in Fig. 10. The results show that the compounds comprise 3–5 bands in the wavelength range from 270 to 600 nm, depending on their molecular structures. There is no reasonable linear absorption in the entire spectral range above 600 nm. The first absorption band of compounds in the region 430–473 nm can be assigned to π–π transition involving the whole electronic system of the compounds with a considerable charge-transfer character originating mainly from the carbazolyl, triphenylamine moieties and pointing towards the heterocoumarin ring which is characterized by a high electron-accepting character. The maximum absorption peaks of the first absorption band are red-shifted from **2t** (439 nm) to **2q** (445 nm), and to **2g** (473 nm), and from **2s** (430 nm) to **2p** (436 nm), and to **2f** (465 nm). It can be seen that the benzocoumarin system caused a bathochromic effect of approximately 400–500 cm^{-1} relative to the coumarin system, suggesting that the conjugation of benzocoumarin ring is larger than that of coumarin skeleton. As a result, the red-shift of absorption can possibly occur. Moreover, replacement of carbazolyl donor with a triphenylamine group in one terminal moiety of the coumarinyl-based molecules resulted in a strong bathochromic shift (1700–1800 cm^{-1}).

In the case of **2e**, the first absorption band was red-shifted to 448 nm, when compared to **2s**, but blue-shifted by about 6 nm with respect to that of AOBO (454 nm) [19] because of steric hindrance resulting from *tert*-butyl.

Note that the absorption profiles and the absorption maxima are mainly dominated by the nature of the excited state π-electron system. As well known, a strong electron donor could help to stabilize the charge-separated excited state of the molecule; the red-shift could be explained by the electron-donating strength of donor group. From the location of the first

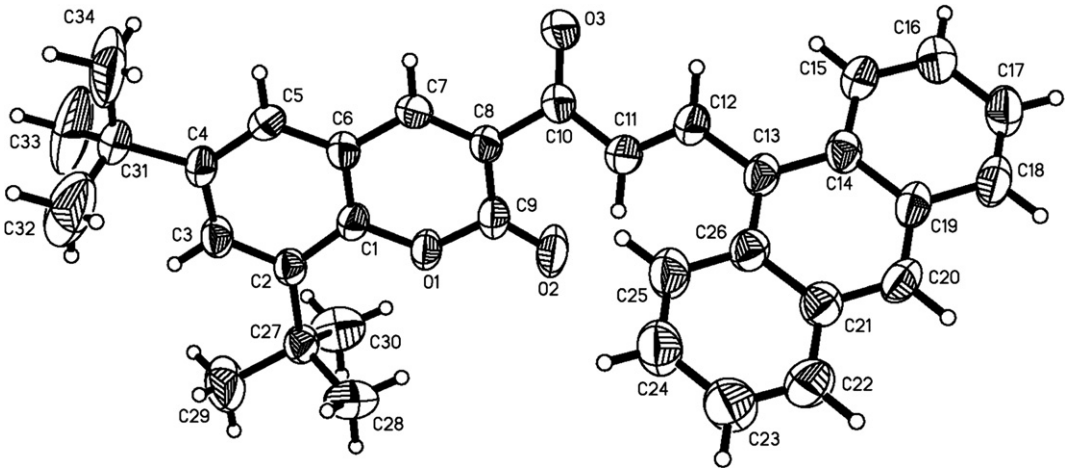

Fig. 6. The molecular structure of **2e**, showing the atom-labelling scheme. Displacement ellipsoids are drawn at the 50% probability level. H atoms are shown as small spheres of arbitrary radius.

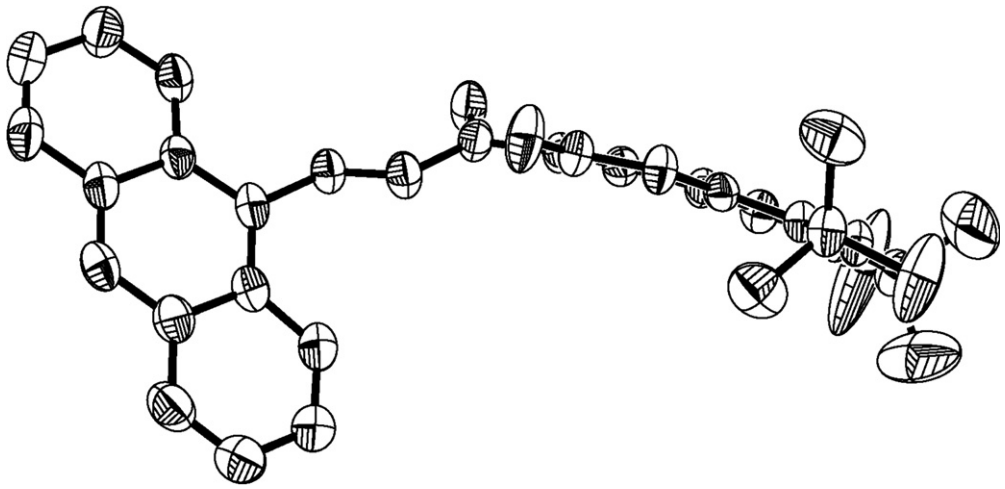

Fig. 7. The side elevation of **2e**. H atoms are omitted for clarity.

absorption band (Fig. 10), the extent of the excited state π-electron system in **2g** seems to be greater than that in others. At the same time, the multi-peak profiles in the linear absorption spectra indicate that molecules in the excited state suffer structure distortions in the π-conjugated frameworks.

The fluorescence spectra for the selected compounds were measured upon the excitation at 360 nm and are presented in Fig. 11. It can be seen from Fig. 11 that the coumarin–chalcone hybrids emit two fluorescence bands. It is similar to that observed in the other families of D–A compounds emitting dual fluorescence [29]. Moreover, all compounds have similar fluorescence spectra. Especially, the similar shape, position and the intense fluorescence peaks, two sharp emission peaks near 410 and 430 nm, were observed for **2e**,

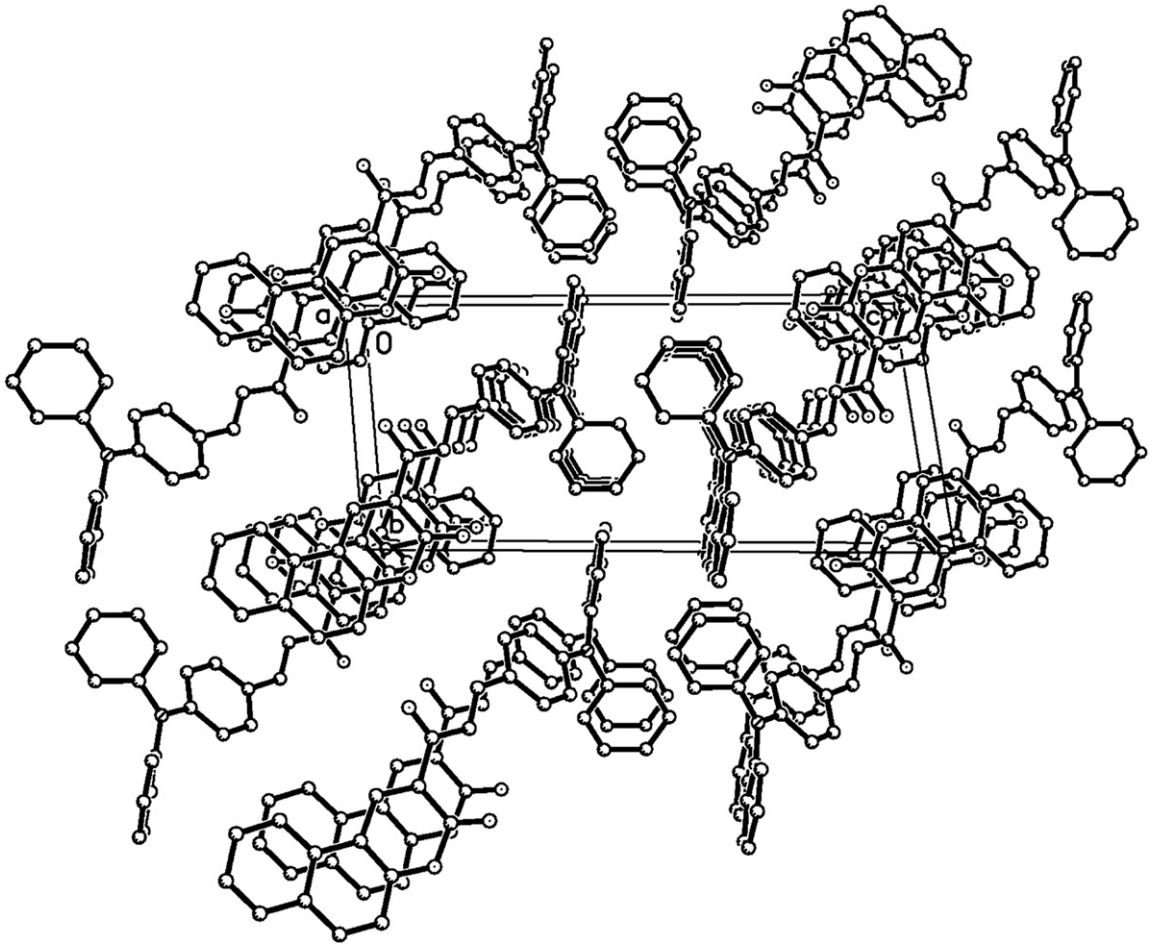

Fig. 8. The packing diagram along *a*-axis of **2g**. H atoms are omitted for clarity.

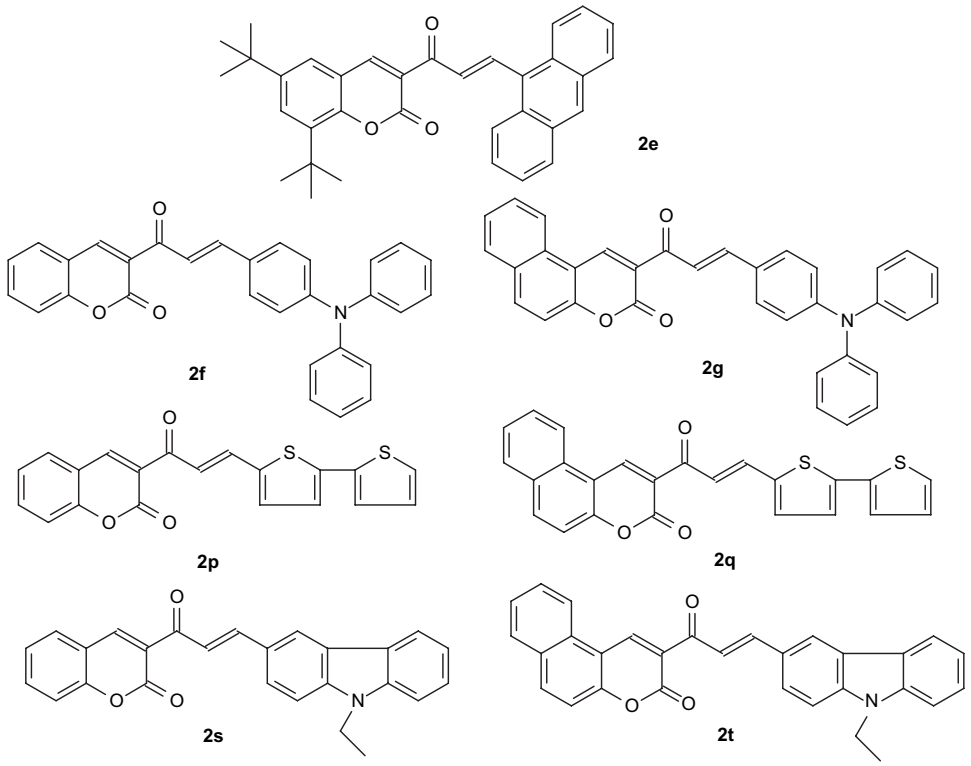

Fig. 9. The molecular structures of the coumarin–chalcone hybrids investigated.

2g, **2p**, **2q**, **2s**, and **2t**, while the corresponding emission peak of **2f** appears around 430 nm, and is the highest and broadest emission peak.

As the remarkable spectral feature of all compounds, it should be noted that the longer wavelength emission obviously causes difference in fluorescence peak position and intensity. Replacing 3-carbonylcoumarin acceptor with a 3-carbonyl-5,6-benzocoumarin, a slightly red-shift fluorescent emission is observed, owing to the larger conjugation of benzocoumarin ring. Similarly, replacement of 2-(thiophen-2-yl)thiophene or carbazolyl groups with a triphenylamine donor, resulted in a strong red-shift fluorescent emission (1700–2000 cm^{-1}). Additionally, among them, **2e** of the anthryl-substituted compound possesses the highest fluorescence intensity, in spite of the shorter emission wavelength (571.5 nm) relative to **2g** (601.5 nm) and **2f** (598 nm).

The results above imply that more π-electrons and longer π-conjugated structure may be involved in **2g** than those in

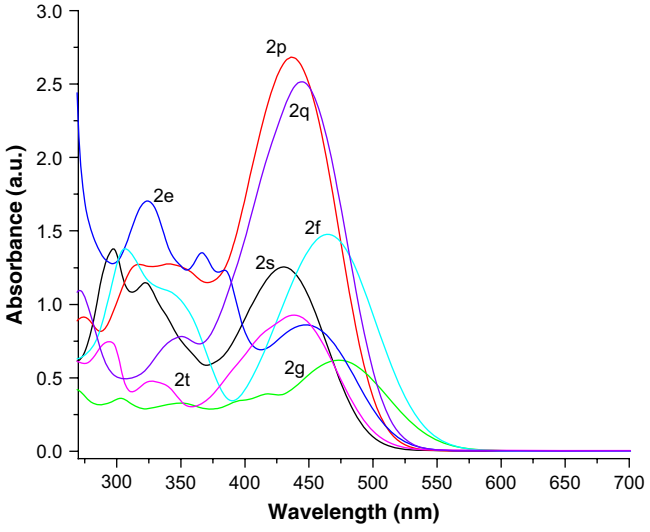

Fig. 10. Absorption spectra of the coumarin–chalcone hybrids in chloroform solution.

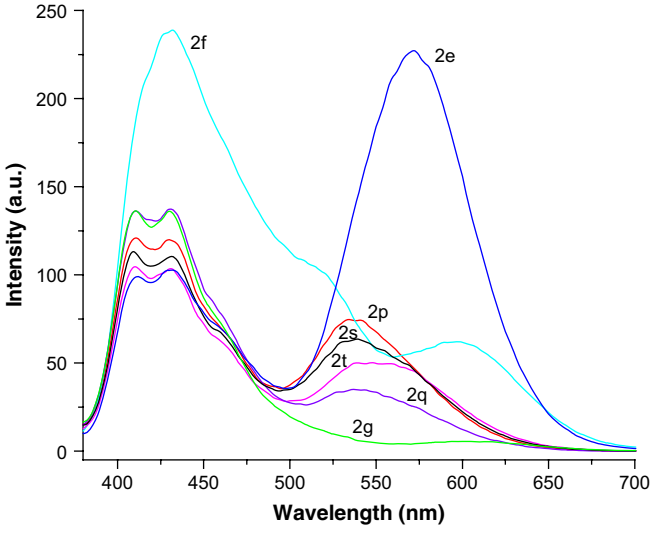

Fig. 11. Fluorescence spectra of the coumarin–chalcone hybrids in chloroform solution.

others. The very weak fluorescence in longer wavelength region for **2g**, with a larger conjugated system and a stronger electron-donating triphenylamine group, may be attributed to both the steric effect and nonemissive twisted intramolecular charge-transfer (TICT) excited state [29].

4. Conclusion

The synthesis and characterization for coumarin-based chromophores containing chalcone moiety are presented in this paper. The crystal structures of **1b**, **1e** and **2g** were investigated by single crystal X-ray crystallography. The absorption and emission spectra of selected coumarin derivatives were studied in solution. It was found that the absorption and emission spectra show red-shift according to the strength of the electron-donating moieties and conjugation length. Replacement of carbazolyl donor with a triphenylamine group in the coumarinyl-based chromophores resulted in a strong bathochromic shift (1700–1900 cm^{-1}), while the benzocoumarin system caused a bathochromic effect of approximately 100–500 cm^{-1} relative to the coumarin system.

It could be expected that this system might be effective for the development of long wavelength emissive chromophores. These coumarinyl-based chromophores could be potential optical materials for some fields, such as OLED materials, two-photon absorption materials, as well as fluorescent probes in biological applications, which are currently being pursued. Further research in this direction is underway in our laboratory.

5. Supplementary material

The crystallographic data (excluding structure factors) of **1b**, **1e** and **2g** have been deposited with the Cambridge Crystallographic Data Center as supplementary publication no. CCDC 649893–649895. Copy of this information may be obtained free of charge via http://www.ccdc.cam.ac.uk or from The Director, CCDC, 12 Union Road, Cambridge CB221EZ, UK (fax: +44 1223/336 033; email: deposit@ccdc.cam.ac.uk). Structural factors are available on request from the authors.

Acknowledgements

This work was supported by the National Natural Science Foundation of China (No. 10374013).

References

[1] Xu GB, Hu DW, Zhao X, Shao ZS, Liu HJ, Tian YP. Fluorescence upconversion properties of a class of improved pyridinium dyes induced by two-photon absorption. Opt Laser Technol 2007;39:690–5.
[2] Mendonca CR, Neves UM, Boni LD, Andrade AA, Santos JDSD, Pavinatto FJ, et al. Two-photon induced anisotropy in PMMA film doped with Disperse Red 13. Opt Commun 2007;273:435–40.
[3] Zhang M, Li MY, Zhao Q, Li FY, Zhang DQ, Zhang JP, et al. Novel Y-type two-photon active fluorophore: synthesis and application in fluorescent sensor for cysteine and homocysteine. Tetrahedron Lett 2007;48:2329–33.
[4] Huang ZL, Li N, Lei H, Qiu ZR, Wang HZ, Zhong ZP, et al. Two-photon induced blue fluorescent emission of heterocycle-based organic molecule. Chem Commun 2002;20:2400–1.
[5] Wang XM, Yang P, Xu GB, Jiang WL, Yang TS. Two-photon absorption and two-photon excited fluorescence of triphenylamine-based multibranched chromophores. Synth Met 2005;155:464–73.
[6] Huang ZZ, Wang XM, Li B, Lu CG, Xu J, Jiang WL, et al. Two-photon absorption of new multibranched chromophores based on bis(diphenylamino)stilbene. Opt Mater 2007;29:1084–90.
[7] Corredor CC, Huang ZL, Belfield KD. Two-photon 3D optical data storage via fluorescence modulation of an efficient fluorene dye by a photochromic diarylethene. Adv Mater 2006;18:2910–4.
[8] Huang ZL, Lei H, Li N, Qiu ZR, Wang HZ, Guo JD, et al. Novel heterocycle-based organic molecules with two-photon induced blue fluorescent emission. J Mater Chem 2003;13:708–11.
[9] Batista RMF, Costa SPG, Malheiro EL, Belsley M, Raposo MMM. Synthesis and characterization of new thienylpyrrolylbenzothiazoles as efficient and thermally stable nonlinear optical chromophores. Tetrahedron 2007;63:4258–65.
[10] Srinivas K, Sitha S, Rao VJ, Bhanuprakash K. Second-order nonlinear response in mono- and di-substituted triazine derivatives: a combined experimental and theoretical analysis. Opt Mater 2006;28:1006–12.
[11] Lee S, Sivakumar K, Shin WS, Xie F, Wang Q. Synthesis and antiangiogenesis activity of coumarin derivatives. Bioorg Med Chem Lett 2006;16:4596–9.
[12] Turki H, Abid S, Fery-Forgues S, Gharbi RE. Optical properties of new fluorescent iminocoumarins: part 1. Dyes Pigments 2007;73:311–6.
[13] Yu TZ, Zhao YL, Ding XS, Fan DW, Qian L, Dong WK. Synthesis, crystal structure and photoluminescent behaviors of 3-(1*H*-benzotriazol-1-yl)-4-methyl-benzo[7,8]coumarin. J Photochem Photobiol A Chem 2007;188:245–51.
[14] Feau C, Klein E, Kerth P, Lebeau L. Synthesis of a coumarin-based europium complex for bioanalyte labeling. Bioorg Med Chem Lett 2007;17:1499–503.
[15] Paula RD, Machado AEDH, Miranda JAD. 3-Benzoxazol-2-yl-7-(*N*,*N*-diethylamino)-chromen-2-one as a fluorescence probe for the investigation of micellar microenvironments. J Photochem Photobiol A Chem 2004;165:109–14.
[16] Kim HM, Fang XZ, Yang PR, Yi JS, Ko YG, Piao MJ, et al. Design of molecular two-photon probes for in vivo imaging. 2*H*-Benzo[*h*]chromene-2-one derivatives. Tetrahedron Lett 2007;48:2791–5.
[17] Jaung JY, Matsuoka M, Fukunishi K. Dicyanopyrazine studies. Part V: syntheses and characteristics of chalcone analogues of dicyanopyrazine. Dyes Pigments 1998;40:11–20.
[18] Li X, Zhao YX, Wang T, Shi MQ, Wu FP. Coumarin derivatives with enhanced two-photon absorption cross-sections. Dyes Pigments 2007;74:108–12.
[19] Huang ZL, Li N, Sun YF, Wang HZ, Song HC, Xu ZL. Synthesis and structure–photophysical property relationships for two coumarinyl-based two-photon induced fluorescent molecules. J Mol Struct 2003;657:343–50.
[20] Sun YF, Song HC, Li WM, Xu ZL. Synthesis of 1,3,4-oxadiazole derivatives for organic electro-transporting electroluminescent materials. Chin J Org Chem 2003;23:1286–90.
[21] Murata C, Masuda T, Kamochi Y, Todoroki K, Yoshida H, Nohta H, et al. Improvement of fluorescence characteristics of coumarins: syntheses and fluorescence properties of 6-methoxycoumarin and benzocoumarin derivatives as novel fluorophores emitting in the longer wavelength region and their application to analytical reagents. Chem Pharm Bull 2005;53:750–8.
[22] Newkome GR, Paudler WW. Contemporary heterocyclic chemistry. Wiley and Sons; 1982.
[23] Krasovitskii BM, Bolotin BM. Organic luminescent materials. VCH; 1988.
[24] Han HM, Lu CR, Zhang Y, Zhang DC. 3-Acetyl-7-methoxycoumarin. Acta Crystallogr 2005;E61:o1864–6.
[25] Cui YZ, Fang Q, Huang ZL, Xue G, Yu WT, Lei H. Synthesis, structure, intense second harmonic generation of K-shaped s-triazine derivative. Opt Mater 2005;27:1571–5.

[26] Sun YF, Zheng DD, Ma CL. Synthesis and crystal structure of 3-(3-anthracen-9-yl-acryloyl)-6,8-di-*tert*-butylcoumarin. Anal Sci 2005;21: X177–8.

[27] Yu HT, Huang YD, Zhang WX, Matsuura T, Meng JB. Crystal structures of two new compounds containing 2,5-diaryl-1,3,4-oxadiazole and triarylamine units. J Mol Struct 2002;642:53–62.

[28] Hu ZJ, Yang JX, Tian YP, Zhou HP, Tao XT, Xu GB, et al. Synthesis and optical properties of two 2,2′:6′,2″-terpyridyl-based two-photon initiators. J Mol Struct 2007;839:50–7.

[29] Grabowski ZR, Rotkiewicz K, Rettig W. Structural changes accompanying intramolecular electron transfer: focus on twisted intramolecular charge-transfer states and structures. Chem Rev 2003;103:3899–4031.